Removal of anionic dyes from aqueous solutions by an ion-exchanger based on pullulan microspheres

Marieta Constantin [a,*], Ionela Asmarandei [a], Valeria Harabagiu [a], Luminita Ghimici [a], Paolo Ascenzi [b], Gheorghe Fundueanu [a]

[a] "Petru Poni" Institute of Macromolecular Chemistry, Department of Natural Polymers, Bioactive and Biocompatible Materials, Gr. Ghica Voda Alley 41A, 700487 Iasi, Romania
[b] Department of Biology and Interdepartmental Laboratory for Electron Microscopy, University Roma Tre, Viale Guglielmo Marconi 446, I-00146 Roma, Italy

ARTICLE INFO

ABSTRACT

Pullulan-graft-poly(3-acrylamidopropyl trimethylammonium chloride) (P-g-pAPTAC) microspheres were prepared by suspension cross-linking of the pullulan previously grafted with cationic moieties. Adsorption of Azocarmine B by the P-g-pAPTAC microspheres was used as a model to demonstrate the removal of anionic dyes from aqueous solutions. Batch adsorption studies concerning the effect of the contact time, pH, initial dye concentration, temperature, grafting, and the nature of sulfonated anionic dyes on the adsorption kinetics were investigated. Adsorption was shown to be independent of pH. The experimental data best fitted to the pseudo-second order model which provided values of the rate constant k_2 of 1.4×10^{-4} g mg^{-1} min^{-1} for 100 mg L^{-1} solution and of 3.7×10^{-4} g mg^{-1} min^{-1} for 500 mg L^{-1} solution. From the Langmuir isotherm linear equation, the maximum adsorption capacity determined was 113.63 mg of Azocarmine B per gram of adsorbent; the negative value of the free energy change indicated the spontaneous nature of the adsorption process.

1. Introduction

Several industries, such as textile, paper, plastics, and dyestuffs, utilize large volume of water and use chemicals and dyes to color their products; as a consequence they generate a considerable amount of polluted wastewater (Crini, 2006; Pokhrel & Viraraghavan, 2004). Dye wastewater discharge into environmental water bodies deteriorates the water quality, and may cause a major impact on human health due to toxic, carcinogenic, mutagenic, and/or teratogenic effects (Otterburn & Aga, 1985). Wastewaters containing dyes are very difficult to treat, since the dyes are recalcitrant molecules, resistant to aerobic digestion, and stable to oxidizing agents.

Reactive dyes contain one or more reactive groups forming covalent links with oxygen, nitrogen and/or sulfur atoms present in cellulose fibers (hydroxyl groups), protein fibers (amino, hydroxyl,

and mercaptan groups) and polyamides (amino group) and providing great stability to the fabric color (Trotmann, 1984).

Some biological, physical, and chemical methods have been employed for dye wastewater treatment (Forgacs, Cserhati, & Oros, 2004). In practice, no single process provides adequate treatment and a combination of different processes is often used to achieve the desired water quality in the most economical way (Gupta & Suhas, 2009). Thus, there is a need to develop new decoloration methods that are effective and acceptable in industrial use.

It is now recognized that adsorption processes using low-cost adsorbents are effective and economic methods for water decontamination. A large variety of non-conventional adsorbent materials have been obtained to remove dyes (Crini, 2006). Much attention has recently been focused on biosorbent materials such as fungal or bacterial biomass and biopolymers that can be obtained in large quantities and that are harmless to nature. Special attention has been given to polysaccharides such as chitosan (Chiou, Ho, & Li, 2004; Chiou & Li, 2003; Dotto & Pinto, 2011; Rosa, Mauro, Riela, & Favere, 2008) and starch or starch-based materials (Delval et al., 2002; Klimaviciute, Riauka, & Zemaitaitis, 2007; Xu, Wang, Wu, Wang, & Li, 2006).

Polysaccharides in the form of cross-linked beads have supplementary advantages such as fast adsorption kinetics, easily operated, and appealing diffusion properties (Bailey, Olin, Bricka, & Adrian, 1999). Due to the hydrophilic nature of the polysaccharides repeating units, these materials possess a remarkably high swelling

---

capacity in water, and consequently their networks are sufficiently expanded to permit a fast diffusion of the pollutants. Even though neutral cross-linked polysaccharides have good adsorption capacity, this can be improved by grafting various functional groups onto the polymer network or the polymer backbone (Arrascue, Garcia, Horna, & Guibal, 2003; Jeon & Höll, 2003). The insertion of new functional groups on the surface of the beads results in an increase of surface polarity and hydrophilicity and this enhances the adsorption of polar adsorbates and improves the adsorption selectivity for the target pollutant. The grafting of carboxyl groups (Chao, Shyu, Lin, & Mi, 2004), amine functions (Jeon & Höll, 2003), and sulfur compounds (Arrascue et al., 2003; Guibal, Von Offenberg Sweeney, Vincent, & Tobin, 2002) has been regarded as an interesting method for these purposes. After adsorption, the cross-linked materials can also be easily regenerated by washing it with a solvent or by solvent extraction.

Among polysaccharides, pullulan (P) is a promising material for biotechnological applications because it is a biocompatible and biodegradable polymer (Xi et al., 1996). Neutral and ionic pullulan derivatives have been also extensively developed for several applications including coating and packaging material, sizing agent for paper or starch substitute in low-calorie food formulations, and cosmetic emulsions (Deshpande, Rale, & Lynch, 1992; Kulicke & Heinze, 2006; Oku, Yamada, & Hosoya, 1979).

Until now, as far as we could ascertain, no data are available concerning the removal of water-soluble anionic dyes by pullulan derivatives. Here, the preparation and characterization of grafted cationic crosslinked pullulan microspheres and their adsorption properties of sulfonated anionic dyes are reported.

2. Materials and methods

2.1. Materials

Pullulan (P) (Mw = 200,000 g mol^{-1}) was purchased from Hayashibara Lab. Ltd. (Okoyama, Japan). (3-Acrylamidopropyl)-trimethylammonium chloride (APTAC) (75%, w/v in water) was obtained from Sigma–Aldrich (St. Louis, MO, USA). Potassium peroxymonosulfate (KPS), and epichlorohydrin (ECH) were purchased from Fluka (Buchs, Switzerland). Cellulose acetate butyrate (CAB) was purchased from Eastman Inc. (Kingsport, TN, USA). 1,2-Dichloroethane was obtained from Fluka and distilled prior to the use. The acid dyes Azocarmine B (AzB), Acid Orange 7 (AO), Methyl Orange (MO), Ponceau 6R (P6R) and Congo Red (CR) were purchased from Sigma–Aldrich. These chemicals are anionic sulfonated dyes with mono azo and multiple azo bonds, and with various degrees and positions of sulfonation (Table 1). All the other reagents were from Fluka. All chemicals were of analytical grade. Unless stated, all chemicals were used without further purification.

2.2. Instrumental analysis

The copolymer composition was determined by nitrogen elemental analysis and ^{1}H NMR spectroscopy. ^{1}H NMR spectra were recorded on a Bruker Avance DRX 400 NMR (Rheinstetten, Germany), using deuterated water as the solvent. The morphology of adsorbent microspheres was examined by using an environmental scanning electron microscope (ESEM) type Quanta 200 (Netherlands), operating with secondary electrons in low vacuum.

The absorption spectra of dye solutions before and after dye adsorption were recorded by using UV-VIS Specord 200 spectrophotometer (Analytic Jena, Jena, Germany) between 350 and 700 nm. The concentration of dye solutions was determined at the wavelength corresponding to the maximum of absorbance (λ_{max}) (see Table 1).

2.3. Preparation of pullulan-graft-poly(3-acrylamidopropyl trimethylammonium chloride) microspheres

Two copolymers with different contents of cationic groups (14% and 22%) (i.e., pullulan-graft-poly(3-acrylamidopropyl trimethyl-lammonium chloride); P-g-pAPTAC) were synthesized by graft-polymerization of APTAC onto pullulan in aqueous solution, using potassium persulfate as the initiator (Constantin, Fundueanu, Cortesi, Esposito, & Nastruzzi, 2003). The microspheres were prepared in one step by suspension cross-linking of P-g-pAPTAC with ECH as previously reported (Constantin, Mihalcea, Oanea, Harabagiu, & Fundueanu, 2010). Briefly, the cross-linked polysaccharide microspheres were produced using a specially designed reactor fitted with a mechanical stirrer, a condenser, and a thermometer. The dispersion medium was constituted of 50 ml of dichloroethane in which 0.5 g of the dispersion agent CAB was dissolved. A solution containing 2 g of P-g-pAPTAC and 2 g of NaOH in 12 ml of water was heated at 50 °C and dispersed in the organic phase at 450 rpm. The w/o emulsion was stirred for 1 h. After the complete dispersion, 2 ml of ECH were added. Afterwards, the cross-linking reaction was carried out for 20 h at 55 °C. The resulting microspheres were isolated by filtration and rinsed in the reactor successively with dichloroethane, acetone, deionized water, and methanol, and finally dried under vacuum at 60 °C for 24 h.

The reaction parameters and physico-chemical properties of P-g-pAPTAC microspheres obtained in the present study are reported in Table 2.

2.4. Dye adsorption by P-g-pAPTAC microspheres

Adsorption studies were performed at 25 ± 1 °C by the batch technique.

2.4.1. Effect of pH

The effect of pH on the adsorption capacity of P-g-pAPTAC microspheres was investigated as follows. Briefly, 50 mg of P-g-pAPTAC microspheres was added to each dye solution (50 ml; 100 mg L^{-1}) at 25 °C. The pH of the solution (between 3 and 9) was adjusted adding either HCl or NaOH. The dye solutions were collected after 24 h and assayed by UV–Vis spectroscopy.

2.4.2. Effect of initial dye concentration

The effect of the dye concentration on the adsorption capacity of P-g-pAPTAC microspheres was investigated as follows. Briefly, 50 mg of P-g-pAPTAC microspheres was added to each dye solution (50 ml; 100, 300 and 500 mg L^{-1}) at pH 7.0 and 25 °C. Kinetics of dye adsorption onto P-g-pAPTAC microspheres was investigated to determine the time when the adsorption equilibrium was reached and the maximum removal of the dye was obtained.

The amount of dye adsorbed by the microspheres at time t (q_t) was obtained from the difference between the initial concentration of dye and the dye concentration in the supernatant after adsorption; q_t was calculated from the mass balance equation (i.e., Eq. (1)):

$$q_t = \frac{V(C_0 - C_t)}{m} \tag{1}$$

where C_0 and C_t are the initial and final dye concentration (mg L^{-1}), respectively, V is the volume of the dye solution (L), and m is the mass of the adsorbent used (g).

When t corresponds to the equilibrium time (i.e., $C_t = C_e$) $q_t = q_e$, the amount of the adsorbed dye at equilibrium, q_e, was calculated according to Eq. (2):

$$q_e = \frac{V(C_0 - C_e)}{m} \tag{2}$$
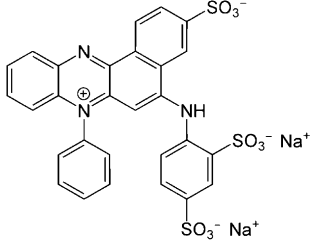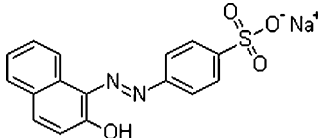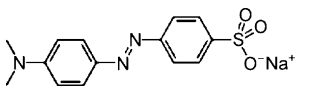
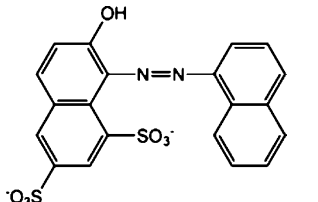**Table 1**
Main characteristics of the acid dyes.
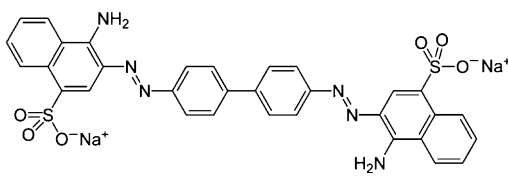
Acid dye	Dye chemical formula	Color index name	Color index number	Molar weight (g mol^{-1})	Charge	λ_{max} (nm)
Azocarmine B (AzB)		50090	Acid Red 103	681.62	−3	516
Acid Orange 7 (AO)		15510	Orange II	350.32	−1	485
Methyl Orange (MO)		13025	Acid Orange 52	327.33	−1	510
Ponceau 6R (P6R)		16250	Acid Red 44	502.44	−2	510
Congo Red (CR)		22120	Direct red 28	696.7	−2	650

Table 2
Reaction parameters and the physico-chemical characteristics of P-g-pAPTAC microspheres.

Sample	Reaction parameters			Microspheres characteristics			
	P-g-pAPTAC concentration (%, w/v)	Crosslinking degree (mol ECH/UG)[c]	pAPTAC content in polymer (wt.%)	E.C.[a] of ms. (mequiv. g^{-1})	pAPTAC content of ms. (wt.%)	Swelling degree (q)[b]	Wrack density (g/ml)
P# 1	20	1.14/1	14	0.72 ± 0.04	13.66	5.4 ± 0.20	0.46 ± 0.02
P# 2	20	1.14/1	22	1.07 ± 0.08	20.14	6.59 ± 0.15	0.33 ± 0.015

[a] E.C., exchange capacity.
[b] $q = V_s/V_d$ (swollen volume/dried volume).
[c] The crosslinking degree is expressed as the molar ratio between ECH and glucose unit of pullulan.

where C_e is the dye concentration at equilibrium (mg L^{-1}).

The amount of adsorbed dye onto microspheres was also calculated as the percentage of removal (R, %) according to Eq. (3):

$$R\,(\%) = \frac{100(C_0 - C_t)}{C_0} \tag{3}$$

2.4.3. Effect of temperature

The effect of temperature on the adsorption capacity of P-g-pAPTAC microspheres was investigated at 25, 35, 45 and 55 °C in a constant temperature shaker bath which controlled the temperature to within ±1 °C. The initial dye concentration was 100 mg L^{-1}.

3. Results and discussion

3.1. Preparation and characterization of the adsorbent

P-g-pAPTAC microspheres were prepared by the suspension cross-linking procedure with ECH (Constantin et al., 2010). The reaction was carried out in a water/organic solvent suspension using a 20% (w/v) aqueous polymer solution (Table 2). P-g-pAPTAC microspheres are characterized by a relative spherical geometry, porous structure and a folded surface architecture (Fig. 1). The size of microspheres ranges between 10 and 300 μm. P-g-pAPTAC microspheres with the diameter ranging between 120 and 250 μm were used for adsorption studies reported below.
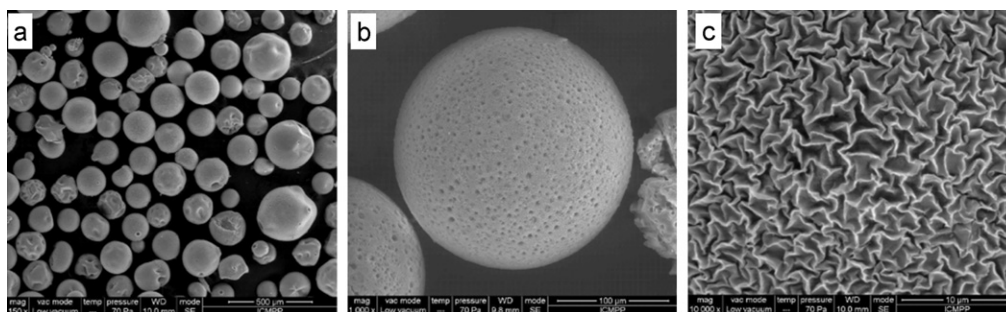
Fig. 1. ESEM photographs of P-g-pAPTAC microspheres. General view (panel a) and surface detail (panel b and c) (sample P# 1 in Table 2).

The total number of amino groups determined by acid–base titration, increases with the amount of poly(3-acrylamidopropyl trimethylammonium chloride) (pAPTAC) in linear polymer (from 0.73 to 1.1 mmol amino groups/g microspheres; samples P# 1 and P# 2 in Table 2, respectively).

The most important factors affecting the adsorption properties of biopolymers are the hydrophilicity and cross-linking density (Crini, 2005; Mocanu, Vizitiu, & Carpov, 2001). In particular, the cross-linked pullulan microspheres possess a high swelling capacity in water due to the hydrophilic nature of their cross-linked units and, consequently, their network is sufficiently expanded to allow a fast diffusion of the adsorbates. On the other hand, cross-linked pullulan grafted with pAPTAC units possesses a hydrophobic character due to the presence of —CH$_2$— units in APTAC. These hydrophobic sites are pivotal in the adsorption of non-polar dyes. Moreover, the network provides a hydrophobic environment into which an apolar pollutant can be trapped; remarkably, the presence of glycosidic oxygen bridges produces a high electron density of the hydrophobic environment (Crini, 2006; Mocanu et al., 2001). This material is also regarded friendly for the environment and less expensive than synthetic commercial resins prepared by using petroleum-based raw materials.

3.2. Kinetics and equilibrium of adsorption

3.2.1. Effect of pH
pH is an important parameter modulating dye adsorption efficiency (Bousher, Shen, & Edyvean, 1997; Ramakrishna & Viraraghavan, 1997). The effect of pH on the adsorption capacity was investigated between pH 3.0 and 9.0, at 25 °C (Fig. 2, panel a). The dye adsorption is unaffected by pH over the whole range explored. In this pH range both the adsorbent and the dye are completely dissociated, because the adsorbent is a strong basic

exchanger and the dye sulfonate is derived from a strong acid; the average value of q_e was 57.48 mg g^{-1}. Similar results were reported for the adsorption of anionic dyes by cross-linked cationic starch (Klimaviciute et al., 2007; Renault, Morin-Crini, Gimbert, Badot, & Crini, 2008) and cross-linked quaternary chitosan (Rosa et al., 2008).

3.2.2. Effect of the adsorbent
In order to study the effect of the adsorbent dosage on dye removal, various amounts of the adsorbent (5–70 mg) were contacted with a fixed initial dye concentration of 100 mg L^{-1}, at pH 7.0 and 25 °C. The removal of the dye increases by increasing the adsorbent dose. In the presence of 70 mg of the adsorbent, almost the complete removal (90%) of the dye was achieved. On increasing the adsorbent dose, additional adsorbent sites become available and hence increasing amounts of the dye are removed from the solution (Fig. 2, panel b). However, on increasing the adsorbent load, the quantity of the dye adsorbed on the unit weight of the adsorbent gets reduced, reflecting the decrease of the q_e value.

A similar behavior was observed for cationic starch derivatives (Khalil & Aly, 2004). Therefore, it could be postulated that the AzB adsorption by cationic pullulan microspheres depended on the amine content.

3.2.3. Effect of the contact time and of the initial dye concentration
The initial concentration of the dye is an important driving force to overcome the mass transfer resistance of the dye from the aqueous and the solid phase. The effect of the initial AzB concentration on the dye removal by P-g-pAPTAC microspheres is shown in Fig. 3. As expected, the overall trend was an increase of the adsorption capacity on increasing the dye concentration; this highlights the strong chemical interaction between the dye molecules and
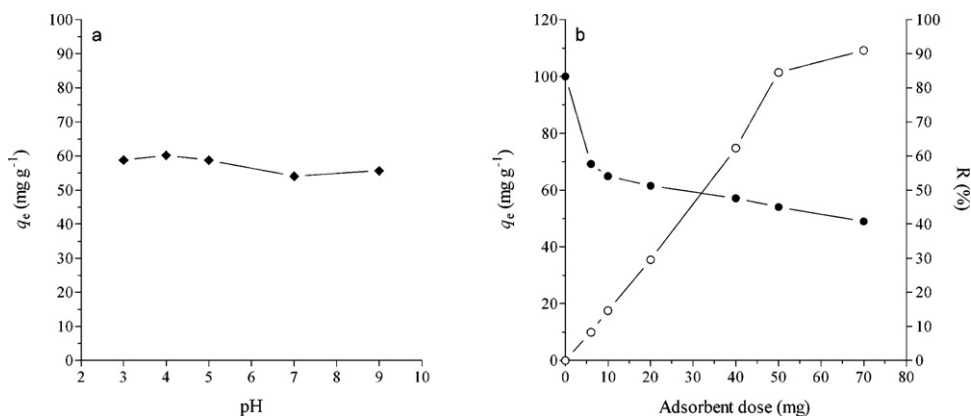

Fig. 2. Effect of the pH (panel a) and of the adsorbent dose (panel b) on the adsorption of AzB by P-g-pAPTAC microspheres, at 25 °C (sample P# 1 in Table 2). [AzB] = 100 mg L^{-1}; contact time = 24 h; shaking rate = 200 rpm. The continuous line is "hand-drawn" line.
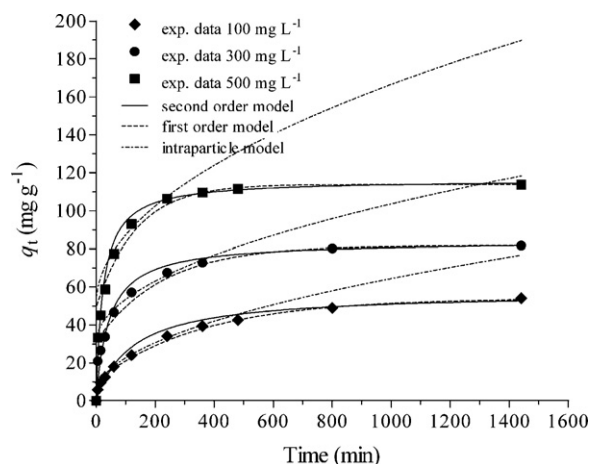
Fig. 3. Comparison between the experimental and theoretical time courses for the adsorption of AzB by P-g-pAPTAC microspheres, at pH 7.0 and 25 °C (sample P# 1 in Table 2). Data were fitted with pseudo-first-order, pseudo-second-order and intra-particle kinetic models according to Eqs. (4)–(6) (see the next section). Adsorbent mass = 50 mg; contact time = 24 h; shaking rate = 200 rpm.

P-g-pAPTAC microspheres. At high dye concentration, the number of sorbate ions which could interact with the available binding sites of the adsorbent increase, hence the dye uptake is enhanced. Values of q_t increase with time, reaching an asymptotic value; under these conditions, no more dye can be removed from the solution. At asymptotic values of q_t, the amount of the dye adsorbed onto the microspheres is in dynamic equilibrium with the amount of the dye desorbed from the adsorbent. The time necessary to reach the asymptotic value of q_t decreases on increasing the dye concentration. Thus, q_t becomes constant after 1440 min, 800 min, and 360 min of shaking at 100, 300, and 500 mg L^{-1} dye concentration, respectively. At longer contact times, the amount of the adsorbed dye remains constant.

3.2.4. Adsorption kinetics

In order to evaluate the kinetic mechanism which controls the dye adsorption by P-g-pAPTAC microspheres (*i.e.*, the pseudo-first-order (Lagergren, 1898) or the pseudo-second-order (Ho & McKay, 1998a, 1998b) or the intra-particle diffusion (Weber & Morris, 1963) model), data given in Fig. 4 were analyzed according to Eqs. (4)–(6):

$$\log(q_e - q_t) = \log q_e - \frac{k_1}{2.303}t \tag{4}$$

$$\frac{t}{q_t} = \frac{1}{k_2 q_e^2} + \frac{1}{q_e}t \tag{5}$$

$$q_t = k_i t^{1/2} + C \tag{6}$$

where q_t and q_e indicate the amount of the adsorbed dye at time t and at equilibrium (mg g^{-1}), respectively; k_1, k_2, and k_i are the pseudo-first order rate constant (min^{-1}), the pseudo-second order rate constant (g mg^{-1} min^{-1}), and the intra-particle diffusion rate constant (mg g^{-1} min$^{-1/2}$) for the adsorption process, respectively; t is time (min); and C is the intercept on the y axis (mg g^{-1}).

Values of parameters obtained from the analysis of data according to the pseudo-first order, the pseudo-second order, and the intra-particle diffusion models are shown in Table 3. To evaluate the most appropriate model fitting the data, the coefficient of determination R^2 was considered.

The experimental data were not well represented by the Lagergren model at all the initial dye concentrations (Fig. 4, panel a). The correlation coefficients values R^2 for the plots are in the 0.9708–0.989 range (Table 3), but the calculated q_e values obtained for this kinetic model are lower than those of the experimental q_e values. This finding suggests that, although R^2 values are reasonably high, the adsorption of AzB onto P-g-pAPTAC microspheres does not follow the pseudo-first order adsorption rate expression postulated by the Lagergren model for the whole adsorption time course. Similar results were previously reported for dyes adsorption onto chitosan (Crini et al., 2008) and cationized starch (Renault et al., 2008).
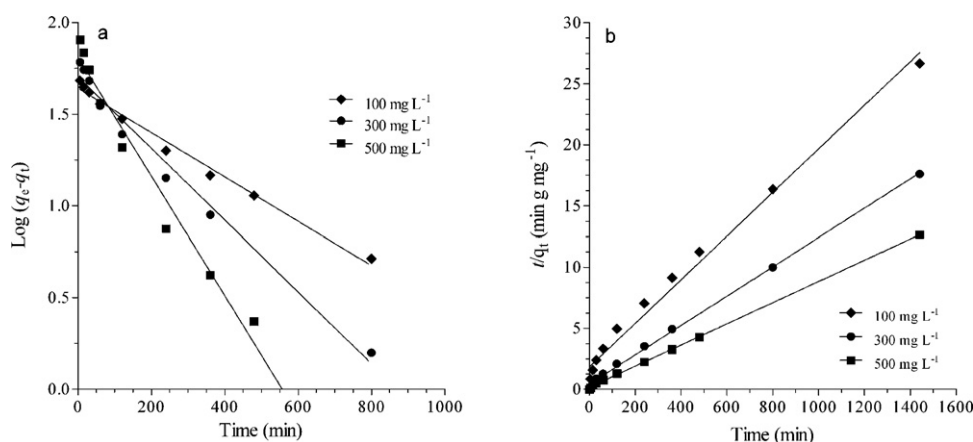

Fig. 4. Lagergren plots (panel a) and pseudo-second-order kinetics (panel b) for AzB adsorption onto P-g-pAPTAC microspheres (sample P# 1 in Table 2), at pH 7.0 and 25 °C. Adsorbent mass = 50 mg; agitation speed = 200 rpm.

Table 3
Effect of the initial dye concentration (C_0) on parameters of kinetic models for AzB adsorption onto P-g-pAPTAC microspheres (sample P# 1 in Table 2) at pH 7.0 and 25 °C. Contact time = 24 h; volume = 50 ml; material mass = 50 mg.

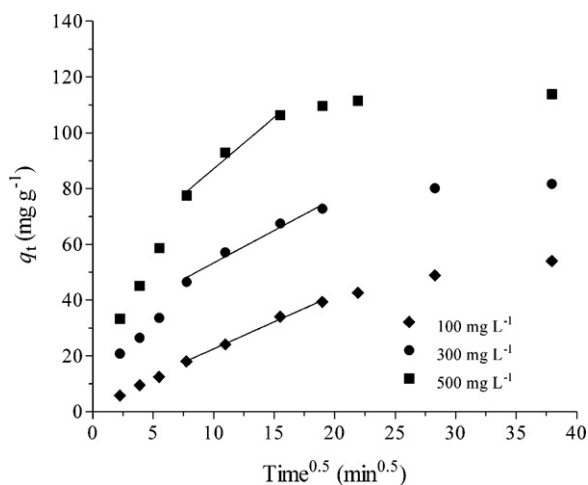| C_0 (mg L^{-1})	$q_{e,exp}$ (mg g^{-1})	Pseudo-first-order			Pseudo-second-order			Intra-particle diffusion		
		k_1 (min^{-1})	$q_{e,calc}$ (mg g^{-1})	R^2	k_2 (g mg^{-1} min^{-1})	$q_{e,calc}$ (mg g^{-1})	R^2	k_i (mg g^{-1} min$^{-1/2}$)	C (mg g^{-1})	R^2
100	54.04	0.002764	43.70	0.9891	0.000143	57.14	0.9911	1.9354	3.21	0.996
300	81.72	0.004606	50.58	0.9826	0.000276	84.03	0.9992	2.3218	30.16	0.978
500	113.83	0.0076	64.744	0.9708	0.000368	116.28	0.9998	3.6715	50.44	0.9796

Fig. 5. Kinetics of AzB adsorption onto P-g-pAPTAC microspheres according the intra-particle diffusion/transport mechanism (sample P# 1 in Table 2), at pH 7.0 and 25 °C. Adsorbent mass = 50 mg; agitation speed = 200 rpm.

Fig. 6. Effect of the poly(APTAC) content of P-g-pAPTAC microspheres on the time course of AzB uptake, at pH 7.0 and 25 °C. Adsorbent mass = 50 mg; [dye] = 500 mg L^{-1}; shaking rate = 200 rpm. The inset shows the pseudo-second-order analysis of the adsorption data.

The plots of t/q_t versus t give a straight line for all the initial dye concentrations studied as shown in Fig. 4, panel b, suggesting the possibility to describe all data sets with the pseudo-second-order model. At all concentrations, R^2 values for the kinetic model were found to be higher (between 0.9911 and 0.9992) than those reported for the Lagergren model; moreover, the calculated and experimental q_e values match very well each other (Table 3). This suggests that the dye adsorption onto P-g-pAPTAC microspheres obeys to the pseudo-second-order kinetic model and supports the assumption that the dye adsorption is due to chemisorption. The dye adsorption takes place *via* surface exchange reactions until the surface functional sites are fully occupied; thereafter, dye molecules bind to the polymer network by a specific recognition and/or reaction.

The adsorbate species are generally transferred from the bulk solution into the solid phase according the intra-particle diffusion/transport mechanism, which represents the rate-limiting step in many adsorption processes, especially in a rapidly stirred batch reactor (Weber & Morris, 1963). As a consequence, the intra-particle diffusion/transport mechanism (Weber & Morris, 1963) was taken into account to determine the rate of dye adsorption onto P-g-pAPTAC microspheres. Fig. 5 shows the time ($t^{1/2}$) dependence of AzB adsorption onto P-g-pAPTAC microspheres at different initial dye concentrations. Data reported in Fig. 5 were not linear over the whole time range, indicating the presence of three steps in the adsorption process. The first step could be attributed to the dye adsorption onto the P-g-pAPTAC microsphere surface, the second step could represent the gradual intra-particle diffusion of the dye, possibly representing the rate limiting step, and the third step could be attributed to the final apparent equilibrium process reflecting the intra-particle diffusion slowing down due to lowering of the dye concentration in solution. It can be observed that the plots do not pass through the origin of axes; in fact, the constant C increases on increasing the AzB concentration (Table 3). This indicates the increase of the thickness of the boundary layer and the decrease of the external mass transfer, *i.e.* the increase of the internal mass transfer. The R^2 values given in Table 3 are close to unity indicating that this model could describe AzB adsorption onto P-g-pAPTAC microspheres. This could indicate that the rate-limiting step is the intra-particle diffusion process, and that the intra-particle diffusion could play a significant role in the uptake of the adsorbate (*i.e.*, AzB) by the adsorbent (*i.e.*, P-g-pAPTAC microspheres).

The analysis of data shown in Table 3 indicates that the linear regression coefficient referring to the pseudo-second order model
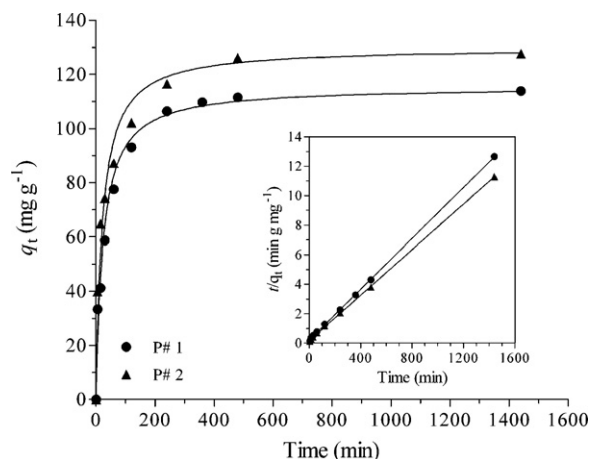
is the best one in describing the adsorption kinetics of dye onto P-g-pAPTAC microspheres. This was also confirmed by data reported in Fig. 3 showing the comparison between the calculated and measured kinetic results.

Further, the effect of the grafting percentage, of temperature, and of the dye characteristics on kinetics was analyzed according to the pseudo-second-order model by Eq. (5). The approaching equilibrium factor (R_W) (Wu, Tseng, Huang, & Juang, 2009), which characterizes kinetics of the adsorption systems, is described by Eq. (7):

$$R_W = \frac{1}{1 + k_s \times q_e \times t_{ref}} \qquad (7)$$

where t_{ref} is the longest operation time of kinetic experiments. The adsorption curve approaches equilibrium when $0.1 < R_W < 1$; it well approaches equilibrium when $0.1 < R_W < 0.01$; and it drastically approaches equilibrium when $R_W < 0.01$ (Wu et al., 2009).

3.2.5. Effect of grafting

To investigate the effect of grafting on dye adsorption onto P-g-pAPTAC microspheres, experiments were conducted at pH 7.0, mixing 50 ml of AzB (500 mg L^{-1}) with 50 mg of grafted microspheres characterized by two different grafting percentages. The results are shown in Fig. 6, the linear plots given in the inset validate of the applicability of the pseudo-second-order model to the dye adsorption kinetics. Data reported in Fig. 6 indicate that the percentage of the AzB adsorption onto P-g-pAPTAC microspheres increases on the grafting percentage, from 113.83 to 127.58 mg g^{-1} (Table 4) as the poly(APTAC) content in the polymer increases from 14 to 22% (wt.).

3.2.6. Effect of temperature

It is well known that temperature plays an important role in ligand adsorption by biopolymers, generally having a negative influence on the ligand amount adsorbed. In fact, temperature can affect several aspects of ligand adsorption such as the dye solubility, the swelling capacity of the adsorbent, and the equilibrium point reflecting the exothermicity of the adsorption phenomenon (Baouab, Gauthier, Gauthier, & Rammah, 2001; Cestari, Vieira, dos Santos, Mota, & deAlmeida, 2004).

Fig. 7 shows the effect of temperatures on AzB adsorption onto P-g-pAPTAC microspheres. The removal of AzB by adsorption onto grafted microspheres decreases from 113.83 mg g^{-1} to

Table 4
Effect of grafting, temperature and of the dye nature on values of kinetic parameters for dye uptake onto P-g-pAPTAC microspheres, at pH 7.0.

Effect of grafting (adsorbent mass = 50 mg; [AzB] = 500 mg L^{-1}; shaking rate = 200 rpm)

Samples	$q_{e,exp}$ (mg g^{-1})	$q_{e,calc}$ (mg g^{-1})	k_2 (g mg^{-1} min^{-1})	R^2	R_W
P# 1	113.83	116.28	0.000359	0.9998	0.01637
P# 2	127.58	129.87	0.000356	0.9997	0.014803

Effect of temperature (adsorbent mass = 50 mg; [AzB] = 500 mg L^{-1}; shaking rate = 200 rpm)

Temperature (°C)	$q_{e,exp}$ (mg g^{-1})	$q_{e,calc}$ (mg g^{-1})	k_2 (g mg^{-1} min^{-1})	R^2	R_W
25	113.83	116.28	0.000359	0.9998	0.01637
35	89.75	90.09	0.001296	0.9998	0.005915
45	76.504	76.92	0.00223	0.9996	0.004033
55	72.08	72.46	0.001035	0.9994	0.009174

Effect of dye nature (adsorbent mass = 50 mg; [dye] = 100 mg L^{-1}; shaking rate = 200 rpm)

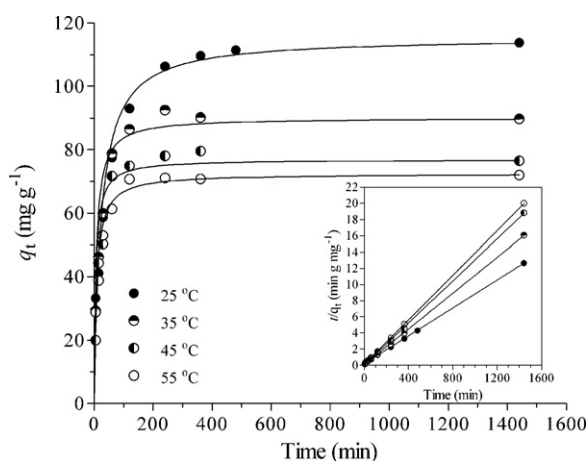| Dye (mol. wt.) (g mol^{-1})	$q_{e,exp}$ (mg g^{-1})	$q_{e,calc}$ (mg g^{-1})	k_2 (g mg^{-1} min^{-1})	R^2	R_W
AO (350.32)	65.42	66.66	0.000782	0.9994	0.01314
MO (327.33)	55.19	55.86	0.001011	0.9999	0.008544
P6R (502.44)	48.14	48.78	0.001652	0.9995	0.012141
AzB (681.62)	54.04	57.14	0.000143	0.9911	0.078381
CR (696.7)	38.18	45.045	0.00007879	0.9921	0.163633

Fig. 7. Effect of temperature on AzB adsorption onto P-g-p(APTAC) microspheres, at pH 7.0 (sample P# 1 in Table 2). Adsorbent mass = 50 mg; [dye] = 500 mg L^{-1}; shaking rate = 200 rpm. The inset shows the pseudo-second-order analysis of the adsorption data.

72.46 mg g^{-1} when temperature increases from 25 to 55 °C, indicating an exothermic process. On the contrary, equilibria were attained in a shorter time at high temperature (*i.e.*, the adsorption equilibria were attained at different contact times). Notably, AzB contains three —SO$_3^-$ groups interacting electrostatically with quaternary ammonium groups present on the adsorbent (*i.e.*, P-g-pAPTAC microspheres). The diffusion of the dye into the microsphere pores is more difficult, since the AzB aromatic chains are ramified and bulky. Therefore, the AzB adsorption seems to occur only onto the surface of the microspheres, and the dye diffusion into the microspheres, which is influenced by the temperature, is neglected. Therefore, at high temperatures, the AzB desorption process appears to be more effective than at low temperatures.

3.2.7. Effect of the dye structure

The adsorption kinetics of five different dyes, Azocarmine B (AzB), Acid Orange 7 (AO), Methyl Orange (MO), Ponceau 6R (P6R), and Congo Red (CR), onto P-g-p(APTAC) microspheres were compared by the pseudo second-order model (the chemical structures of dyes are reported in Table 1).

The adsorption process is electrostatically driven by the counterions present in the adsorbent and in the dye. Therefore, the difference in the degree of dyes adsorption could reflect their structure. In fact, the relative order of the adsorption capacity of the dyes considered (CR < P6R < MO < AzB < AO) does not agree with the relative order of the number of their charges (AO = MO < CR = P6R < AzB). Notably, AO and MO contain one sulfonic group (see Table 1), but different aromatic substituents; in fact, AO and MO contain a naphthalene ring and a benzene ring, respectively. As shown in Fig. 8, the adsorption capacity of AO onto P-g-p(APTAC) microspheres is higher than that of MO indicating that bulkier is the aromating substituent greater is the binding force of the dye. This indicates that also hydrophobic contributions could play a significant role in the binding of the dye by polycations; indeed AO and MO display the same ionic group (see Table 1). Table 4 shows that a higher quantity of the divalent compound P6R is adsorbed on P-g-p(APTAC) microspheres than CR, suggesting that bulky portions of these dyes (see Table 1) do not enter or partly penetrate P-g-p(APTAC) microspheres, thus, dyes preferentially adsorb at the outer surface of microspheres. Notably, a similar behavior has been reported for chitin adsorbent (Wong, Szeto, Cheung, & McKay, 2003). Lastly, AzB which has a quinone-imine structure and three sulfonic groups (see Table 1) displays the highest adsorption capacity, probably due to his bulky non-polar portion (Table 4).

3.3. Adsorption isotherm

Adsorption properties and equilibrium data illustrate how adsorbate molecules (pollutants) interact with adsorbent and thus are very important to optimize the use of pullulan microspheres (Allen, McKay, & Porter, 2004; Tien, 1994). The distribution of the dye molecules between the liquid phase and the adsorbent is a measure of the equilibrium state occurring in the adsorption process and can generally be expressed by one or more series of isotherm models. The isotherm shape can provide qualitative information on the nature of the solute–surface interaction (Al-Duri, 1996; Tien, 1994). Two isotherms (Langmuir and Freundlich isotherms) were used to fit the experimental data. The Langmuir equation is based on the assumption that a structurally homogenous adsorbent displays multiple, identical, and energetically equivalent adsorption sites (Cvetkovic, Straathof, Krishna, & Van der Wielen, 2005; Langmuir, 1918). The Langmuir model is described by Eq. (8):

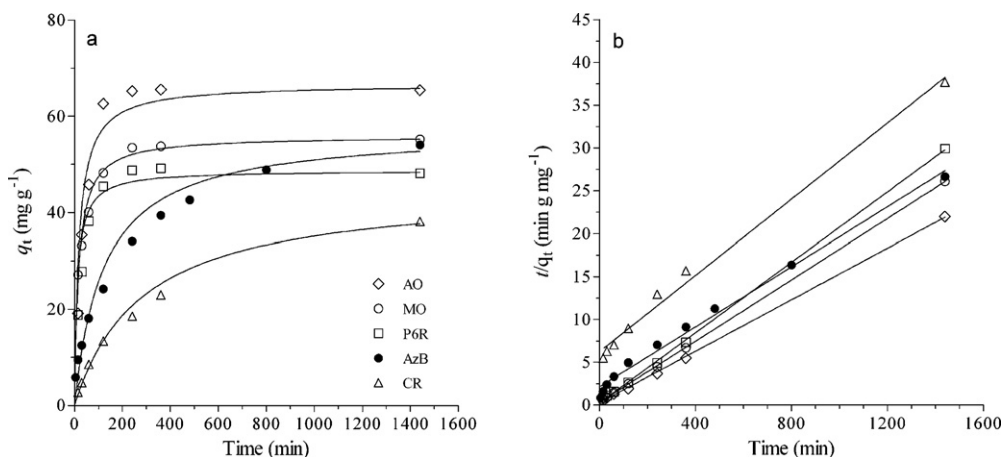$$q_e = \frac{K_L C_e}{1 + a_L C_e} \qquad (8)$$

Fig. 8. Effect of the dye structure on the adsorption onto P-g-p(APTAC) microspheres (panel a) and the pseudo-second-order model for the analysis of the adsorption data (panel b), at pH 7.0 and 25 °C (sample P# 1 in Table 1). Adsorbent mass = 50 mg; [dye] = 100 mg L^{-1}; shaking rate = 200 rpm.

where q_e is the solid phase adsorbate concentration at equilibrium (mg g^{-1}), C_e is the aqueous phase adsorbate concentration at equilibrium (mg L^{-1}), and K_L (L g^{-1}) and a_L (L mg^{-1}) are the Langmuir isotherm constants. Eq. (8) could be rearranged as shown in Eq. (9):

$$\frac{C_e}{q_e} = \frac{1}{K_L} + \frac{a_L}{K_L} C_e \tag{9}$$

The plot of C_e/q_e versus C_e gives a straight line with the slope a_L/K_L and the y-intercept $1/K_L$. The maximum adsorption capacity of the adsorbent (q_m) corresponds to K_L/a_L.

The Freundlich isotherm describes heterogeneous systems, i.e., compounds with adsorbent surfaces with non-energetically equivalent binding sites (Freundlich, 1906). The Freundlich model is described by the empirical Eq. (10):

$$q_e = K_F C_e^{1/n_F} \tag{10}$$

where K_F is the Freundlich constant being indicative of the extent of adsorption, and $1/n_F$ is the heterogeneity factor being an indicator of adsorption effectiveness and of the deviation from linearity of the adsorption process. The $1/n_F$ value ranges between 0 and 1, and indicates the degree of non-linearity between the solution concentration of the dye and the dye adsorption. When the value of $1/n_F$ is equal to unity, the adsorption is linear; when the value of $1/n_F$ is below the unity, the adsorption process is chemically driven; and when the value of $1/n_F$ is above the unity, adsorption is a physically driven process. The more heterogeneous is the adsorbent surface, closer is the $1/n_F$ value approaching to 0 (Al-Duri, 1996).

The relationship between the amount of AzB adsorbed onto microspheres at the adsorbent surface and the dye concentration present in the aqueous phase at equilibrium is shown in Fig. 9 (panel c). The analysis of data demonstrated that the adsorption capacity increases with the dye concentration in solution, reaching progressively the adsorbent saturation. The Langmuir and Freundlich isotherms fitting the experimental data are shown in Fig. 9 (panel c), and the corresponding parameters are listed in Table 5.

3.3.1. Langmuir isotherm

The linearized form of the Langmuir isotherm (Fig. 9, panel a) fits all data determined over the whole concentration range explored, the correlation coefficient was 0.9992 (see Table 5). The value of the correlation coefficient strongly supports the fact that the AzB adsorption data closely follow the Langmuir model. The isotherm constants, a_L, K_L and equilibrium monolayer capacities, q_m are reported in Table 5. The high value of a_L indicated a strong binding capacity. The Langmuir monolayer capacity q_m represents the saturation capacity of AzB, its value being 113.63 mg of AzB per gram of

polymer indicates that P-g-pAPTAC microspheres exhibit relevant adsorption properties.

The good agreement between the experimental and calculated values of q_e according to the Langmuir model (see Fig. 9, panel c) indicates that AzB forms monolayer coverage onto the adsorbent surface. The high degree of correlation for the linearized Langmuir relationship (Fig. 9, panel a) suggests that the single surface chemisorption is the predominant process and possibly represents the rate controlling step. The essential feature of the Langmuir isotherm can be expressed in terms of a dimensionless constant called separation factor (R_L, also named equilibrium parameter) which is defined by Eq. (11) (Hall, Eagleton, Acrivos, & Vermeulen, 1966):

$$R_L = \frac{1}{1 + a_L C_0} \tag{11}$$

where C_0 is the initial concentration (mg L^{-1}) and a_L is the Langmuir constant related to the energy of adsorption (L mg^{-1}). The value of R_L indicates the shape of the Langmuir isotherm which can be either unfavorable ($R_L > 1$) or linear ($R_L = 1$) or favorable ($0 < R_L < 1$) or irreversible ($R_L = 0$) (Webi & Chakravort, 1974).

The value of R_L for AzB adsorption onto P-g-pAPTAC microspheres ranges between 0.036 and 0.431 (Table 5) confirming the favorable uptake of the dye.

Table 6 lists the comparison of maximum adsorption capacity of some anionic dyes on various polysaccharide-based adsorbents reported in the literature. Compared with these data, the cross-linked P-g-p(APTAC) microspheres studied in this work are effective in the adsorption of anionic dyes from aqueous solutions, having promising potential as adsorbents for environmental field applications.

3.3.2. Freundlich isotherm

The inspection of the linear Freundlich isotherm plots (Fig. 9, panel c) suggests that the Langmuir model allows a much better analysis of data than the Freundlich model. In fact, Fig. 9 (panel b) exhibits a deviation from linearity of the Freundlich linear plot for the whole concentration ranges. However, if the whole concentration range is divided into regions, i.e., region 1 and region 2, a good data fit appears to occur at the low dye concentration. According to literature (Wong et al., 2003), this may reflect the irregular energy distribution on the adsorbent surface due to the presence of different groups (i.e., hydroxyl groups and quaternary ammonium, respectively) with different activation energies. Table 5 shows the Freundlich adsorption isotherm constants, n_F and K_F, and the correlation coefficients, R^2 for the low and high concentration ranges.
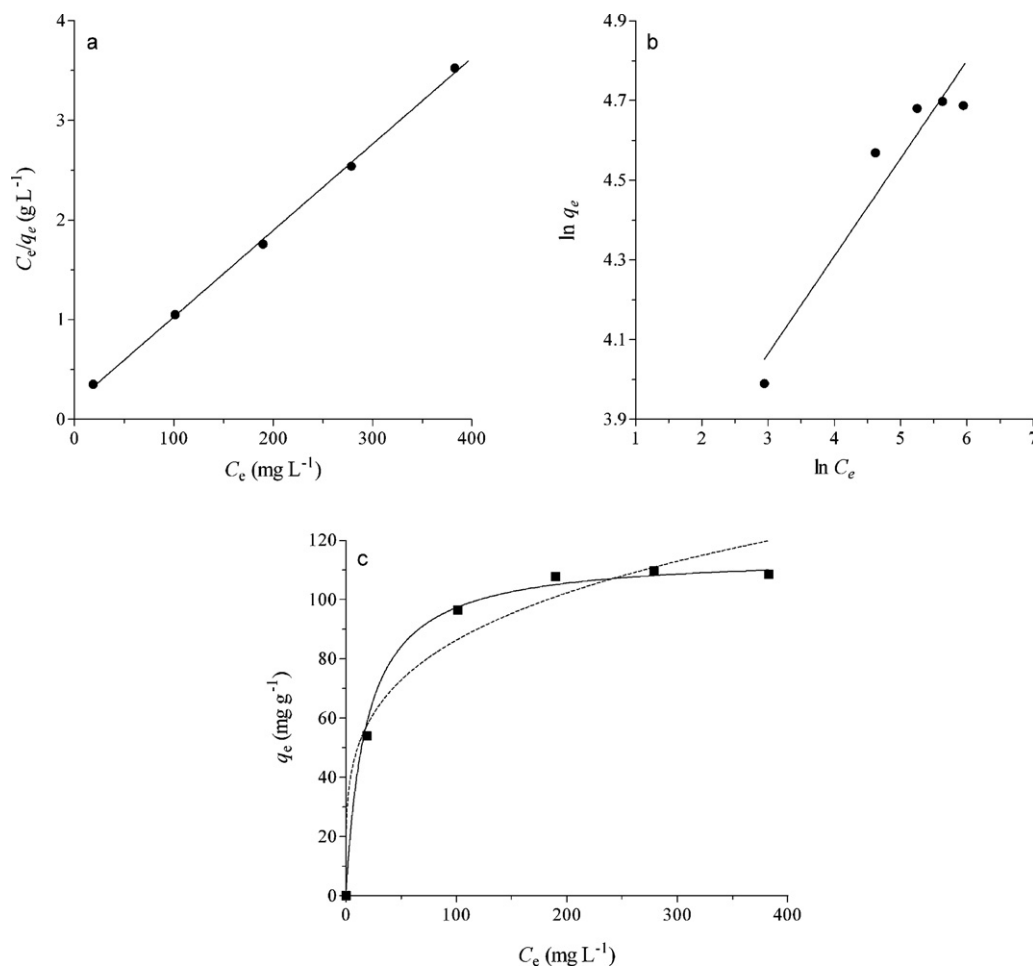
Fig. 9. Langmuir (panel a) and Freundlich (panel b) models describing the adsorption of AzB onto P-g-pAPTAC microspheres (sample P# 1 in Table 2), at pH 7.0 and 25 °C; Adsorption isotherms (panel c) fitted by the Langmuir (continuous line) and Freundlich (dashed line) models.

Table 5
Parameters describing AzB adsorption onto P-g-pAPTAC microspheres according the Langmuir and Freundlich models, at pH 7.0 and 25 °C.

Langmuir model					Freundlich model			
a_L (Lmg^{-1})	K_L (Lg^{-1})	q_m (mgg^{-1})	R^2	R_L	Region of the Freundlich's curve	n_F	K_F (Lmg^{-1})	R^2
					Low concentration	4.105	31.299	1
0.06945	7.89	113.63	0.9992	0.036–0.431	High concentration	87.719	101.962	0.2037
					Whole concentration range	5.359	38.436	0.9399

At the high dye concentration, the Freundlich equation does not fit the experimental data. At low dye concentration, the Freundlich isotherm parameter is lower than 1 ($1/n_F = 0.2436$), indicating that AzB is favorably adsorbed by the adsorbent, a condition that does not apply at high dye concentrations.

3.4. Thermodynamic parameters

Values of the Gibbs free energy ($\Delta G°$), the enthalpy change ($\Delta H°$), and entropy ($\Delta S°$) were calculated according the van't Hoff equation (Eq. (12)):

$$\ln K_{eq} = -\frac{\Delta H°}{RT} + \frac{\Delta S°}{R} \tag{12}$$

$$K_{eq} = \frac{q_e}{C_e} \tag{13}$$

where K_{eq} is the equilibrium constant, q_e is the amount of adsorbed dye at equilibrium (mg g^{-1}), C_e is the concentration of the unbound dye at equilibrium (mg L^{-1}), R is the ideal gas constant (8.314 J K^{-1} mol^{-1}) and T is the temperature in Kelvin.

Experiments were carried out between 298 and 328 K, and the change in free energy was calculated according to Eq. (14):

$$\Delta G° = -RT \ln K_{eq} \tag{14}$$

Values of ΔH and ΔS (Table 7) were calculated from the slope and intercept of van't Hoff plots of $\ln K_{eq}$ versus $1/T$.

All values of $\Delta G°$ are negative independently of temperature, confirming the feasibility and spontaneous nature of the adsorption process under all the experimental conditions. The decrease of ΔG values on increasing temperature suggests that the AzB adsorption is impaired at high temperatures.

The negative $\Delta H°$ value (-21.163 kJ mol^{-1}) indicates that the dye adsorption is an exothermic process, while the negative $\Delta S°$ value indicates a scarce disorder at the solid–solution interface during dye adsorption. As the temperature goes up, the mobility of the dye molecules increases, causing the molecules to escape from the solid phase to the liquid phase, this leads to the decrease

Table 6
Reported maximum adsorption capacities (q_m) in the literature for some anionic dyes obtained on polysaccharide-based materials.

Adsorbent	Dye	pH	q_m (mg g^{-1})	References
Crosslinked starch				
Cationized with quaternary ammonium groups	Acid Blue 25	6	322	Renault et al. (2008)
		–	249	Delval et al. (2002)
	Acid Red 151	–	367–1461	Klimaviciute et al. (2007)
	Acid Blue 25	–	366–778	
Amphoteric with carboxymethyl and quaternary ammonium groups	Acid Light Yellow 2G	–	227.27	Xu et al. (2006)
	Acid Red G		217.39	
Ethylenediamine modified starch	Acid Orange 10	4	267.3	Cheng, Ou, Li, Li, and Xiang (2009)
	Acid Green 25		513.5	
	Amido Black 10B		656.8	
Methylene dimethylamine hydrochloride modified starch	Reactive brilliant red KE-3B	5	209	Jiang, Ju, Zhang, and Yang (2010)
Crosslinked chitosan (beads)	Congo Red	5	208.3	Chatterjee, Chatterjee, and Woo (2010)
			209	Chatterjee, Chatterjee, and Woo (2011a)
	Eosin Y (Acid red 87)	6	81	Chatterjee, Chatterjee, Chatterjee, and Das (2005)
Ethylenediamine modified chitosan	Eosin Y	5	294.12	Huang et al. (2011)
Poly(ethyleneimine)-grafted chitosan	Reactive Black 5	6	413	Chatterjee, Chatterjee, and Woo (2011b)
Non-crosslinked				
Poly(methyl methacrylate) grafted chitosan	Procion Yellow MX	7	250	Singh, Sharma, Tripathi, and Sangh (2009)
	Remazol Brilliant Violet		357	
	Reactive Blue H5G		178	
Poly(alkyl methacrylate)s grafted chitosan	Orange G	7	265–435	Konaganti, Kota, Patil, and Madras (2010)
Crosslinked poly(acrylamidopropyl trimethylammonium) grafted pullulan	Azocarmine B	7	113.6	Present work

Table 7
Thermodynamic parameters for the adsorption of AzB onto P-g-pAPTAC microspheres (sample P# 1 in Table 2).

Temperature (K)	ΔG (kJ mol^{-1})	ΔH (kJ mol^{-1})	ΔS (J K^{-1} mol^{-1})	R^2
298	−3.017			
303	−2.855	−21.163	−60.67	0.9932
313	−2.188			
323	−1.537			

of the adsorption capacity of AzB. Similar results agree with those previously reported concerning the adsorption of acid dyes onto cross-linked chitosan beads (Kamari, Wan Ngah, Chong, & Cheah, 2009) and of anionic dye eosin Y onto ethylenediamine-modified chitosan (Huang, Bin, Bu, Jiang, & Zeng, 2011).

4. Conclusions

The performance of the pullulan-graft-poly(APTAC) microspheres as an adsorbent to remove acid dyes from aqueous solution has been investigated. The results indicate that the adsorption process is independent of pH since the most probable mechanism for adsorption is the interaction of the polymer quaternary ammonium groups with the sulfonate groups of dyes. Equilibrium isotherms and kinetic models have been considered to assess the dye adsorption capacity of grafted pullulan microspheres. Adsorption kinetics follows the pseudo-second-order mechanism and adsorption equilibria are satisfactorily fitted by the Langmuir equation; the maximum adsorption capacity of pullulan-graft-poly(APTAC) microspheres is 113.63 mg g^{-1}.

References

Al-Duri, B. (1996). Adsorption modeling and mass transfer. In G. McKay (Ed.), *Use of adsorbents for the removal of pollutants from wastewaters* (pp. 133–173). London: CRC Press.

Allen, S. J., McKay, G., & Porter, J. F. (2004). Adsorption isotherm models for basic dye adsorption by peat in single and binary component systems. *Journal of Colloid and Interface Science*, 280, 322–333.

Arrascue, M. L., Garcia, H. M., Horna, O., & Guibal, E. (2003). Gold sorption on chitosan derivatives. *Hydrometallurgy*, 71, 191–200.

Bailey, S. E., Olin, T. J., Bricka, R. M., & Adrian, D. D. (1999). A review of potentially low-cost sorbents for heavy metals. *Water Research*, 33, 2469–2479.

Baouab, M. H. V., Gauthier, R., Gauthier, H., & Rammah, M. E. B. (2001). Cationized sawdust as ion exchanger for anionic residual dyes. *Journal of Applied Polymer Science*, 82, 31–37.

Bousher, A., Shen, X., & Edyvean, R. G. J. (1997). Removal of coloured organic matter by adsorption onto low-cost waste materials. *Water Research*, 31, 2084–2092.

Cestari, A. R., Vieira, A. F. S., dos Santos, A. G. P., Mota, J. A., & deAlmeida, V. P. (2004). Adsorption of anionic dyes on chitosan beads. 1. The influence of the chemical structures and temperature on the adsorption kinetics. *Journal of Colloid and Interface Science*, 280, 4905–4909.

Chao, A. C., Shyu, S. S., Lin, Y. C., & Mi, F. L. (2004). Enzymatic grafting of carboxyl groups on to chitosan—To confer on chitosan the property of a cationic dye adsorbent. *Bioresource Technology*, 91, 157–162.

Chatterjee, S., Chatterjee, S., Chatterjee, B. P., & Das, A. R. (2005). Adsorption of a model anionic dye, eosin Y, from aqueous solution by chitosan hydrobeads. *Journal of Colloid and Interface Science*, 288, 30–35.

Chatterjee, S., Chatterjee, T., & Woo, S. H. (2010). A new type of chitosan hydrogel sorbent generated by anionic surfactant gelation. *Bioresource Technology*, 101, 3853–3858.

Chatterjee, S., Chatterjee, T., & Woo, S. H. (2011a). Adsorption of Congo Red from aqueous solutions using chitosan hydrogel beads formed by various anionic surfactants. *Separation Science and Technology*, 46, 986–996.

Chatterjee, S., Chatterjee, T., & Woo, S. H. (2011b). Influence of the polyethyleneimine grafting on the adsorption capacity of chitosan beads for Reactive Black 5 from aqueous solutions. *Chemical Engineering Journal*, 166, 168–175.

Cheng, R., Ou, S., Li, M., Li, Y., & Xiang, B. (2009). Ethylenediamine modified starch as biosorbent for acid dyes. *Journal of Hazardous Materials*, 172, 1665–1670.

Chiou, M. S., Ho, P. Y., & Li, H. Y. (2004). Adsorption of anionic dyes in acid solutions using chemically cross-linked chitosan beads. *Dyes and Pigments*, 60, 69–84.

Chiou, M. S., & Li, H. Y. (2003). Adsorption behavior of reactive dye in aqueous solution on chemical cross-linked chitosan beads. *Chemosphere*, 50, 1095–1105.

Constantin, M., Fundueanu, G., Cortesi, R., Esposito, E., & Nastruzzi, C. (2003). Aminated polysaccharide microspheres as DNA delivery systems. *Drug Delivery*, 10, 139–149.

Constantin, M., Mihalcea, I., Oanea, I., Harabagiu, V., & Fundueanu, G. (2010). Studies on graft copolymerization of 3-acrylamidopropyl trimethylammonium chloride on pullulan. *Carbohydrate Polymers*, 84, 926–932.

Crini, G. (2005). Recent developments in polysaccharide-based materials used as adsorbents in wastewater treatment. *Progress in Polymer Science*, 30, 38–70.

Crini, G. (2006). Non-conventional low-cost adsorbents for dye removal: A review. *Bioresource Technology*, *97*, 1061–1085.

Crini, G., Gimbert, F., Robert, C., Martel, B., Adam, O., Morin-Crini, N., et al. (2008). The removal of Basic Blue 3 from aqueous solutions by chitosan-based adsorbent: Batch studies. *Journal of Hazardous Materials*, *153*, 96–106.

Cvetkovic, A., Straathof, A. J. J., Krishna, R., & Van der Wielen, L. A. M. (2005). Adsorption of xanthene dyes by lysozyme crystals. *Langmuir*, *21*, 1475–1480.

Delval, F., Crini, G., Morin, N., Vebrel, J., Bertini, S., & Torri, G. (2002). The sorption of several types of dye on crosslinked polysaccharides derivatives. *Dyes and Pigments*, *53*, 79–92.

Deshpande, M. S., Rale, V. B., & Lynch, J. M. (1992). Aureobasidium pullulans in applied microbiology: A status report. *Enzyme and Microbial Technology*, *14*, 514–527.

Dotto, G. L., & Pinto, L. A. A. (2011). Adsorption of food dyes onto chitosan: Optimization process and kinetic. *Carbohydrate Polymers*, *84*, 231–238.

Forgacs, E., Cserhati, T., & Oros, G. (2004). Removal of synthetic dyes from wastewaters: A review. *Environment International*, *30*, 953–971.

Freundlich, H. M. F. (1906). Über die adsorptionin lösungen. *Zeitschrift für Physikalische Chemie*, *57*, 385–470.

Guibal, E., Von Offenberg Sweeney, N., Vincent, T., & Tobin, J. M. (2002). Sulfur derivatives of chitosan for palladium sorption. *Reactive and Functional Polymers*, *50*, 149–163.

Gupta, V. K., & Suhas. (2009). Application of low-cost adsorbent for dye removal—A review. *Journal of Environmental Management*, *90*, 2313–2342.

Hall, K. R., Eagleton, L. C., Acrivos, A., & Vermeulen, T. (1966). Pore- and solid-diffusion kinetics in fixed-bed adsorption under constant-pattern conditions. *Industrial & Engineering Chemistry Fundamentals*, *5*, 212–223.

Ho, Y. S., & McKay, G. (1998a). Sorption of dye from aqueous solution by peat. *Chemical Engineering Journal*, *70*, 115–124.

Ho, Y. S., & McKay, G. (1998b). Kinetic models for the sorption of dye from aqueous solution by wood. *Transactions of the Institution of Chemical Engineers*, *76*, 183–191.

Huang, X.-Y., Bin, J.-P., Bu, H.-T., Jiang, G.-B., & Zeng, M.-H. (2011). Removal of anionic dye eosin Y from aqueous solution using ethylenediamine modified chitosan. *Carbohydrate Polymers*, *84*, 1350–1356.

Jeon, C., & Höll, W. H. (2003). Chemical modification of chitosan and equilibrium study for mercury ion removal. *Water Research*, *37*, 4770–4780.

Jiang, Y., Ju, B., Zhang, S., & Yang, J. (2010). Preparation and application of a new cationic starch ether—Starch–methylene dimethylamine hydrochloride. *Carbohydrate Polymers*, *80*, 467–473.

Kamari, A., Wan Ngah, W. S., Chong, M. Y., & Cheah, M. L. (2009). Sorption of acid dyes onto GLA and H$_2$SO$_4$ cross-linked chitosan beads. *Desalination*, *249*, 1180–1189.

Khalil, M. I., & Aly, A. A. (2004). Use of cationic starch derivatives for the removal of anionic dyes from textile effluents. *Journal of Applied Polymer Science*, *93*, 227–234.

Klimaviciute, R., Riauka, A., & Zemaitaitis, A. (2007). The binding of anionic dyes by cross-linked cationic starches. *Journal of Polymer Research*, *14*, 67–73.

Konaganti, V. K., Kota, R., Patil, S., & Madras, G. (2010). Adsorption of anionic dyes on chitosan grafted poly(alkyl methacrylate)s. *Chemical Engineering Journal*, *158*, 393–401.

Kulicke, W. M., & Heinze, T. (2006). Improvements in polysaccharides for use as blood plasma expanders. *Macromolecular Symposia*, *231*, 47–59.

Lagergren, S. (1898). Zur theorie der sogenannten adsorption gelö ester stoffe. *Kungliga Svenska Vetenskapsakademiens Handlingar*, *24*, 1–39.

Langmuir, I. (1918). The adsorption of gases on plane surfaces of glass, mica and platinum. *Journal of the American Chemical Society*, *40*, 1361–1368.

Mocanu, G., Vizitiu, D., & Carpov, A. (2001). Cyclodextrin polymers. *Journal of Bioactive and Compatible Polymers*, *16*, 315–342.

Oku, T., Yamada, K., & Hosoya, N. (1979). Effects of pullulan and cellulose on the gastrointestinal tract of rats. *Nutrition & Food Science*, *32*, 235–241.

Otterburn, M. S., & Aga, D. A. (1985). Fullers earth and fired clay as adsorbent for dye stuffs, equilibrium and rate constants. *Water, Air, & Soil Pollution*, *24*, 307–322.

Pokhrel, D., & Viraraghavan, T. (2004). Treatment of pulp and paper mill wastewater—A review. *Science of the Total Environment*, *333*, 37–58.

Ramakrishna, K. R., & Viraraghavan, T. (1997). Use of slag for dye removal. *Waste Management*, *17*, 483–488.

Renault, F., Morin-Crini, N., Gimbert, F., Badot, P. M., & Crini, G. (2008). Cationized starch-based material as a new ion-exchanger adsorbent for the removal of C.I. Acid Blue 25 from aqueous solutions. *Bioresource Technology*, *99*, 7573–7586.

Rosa, S., Mauro, C. M. L., Riela, H. G., & Favere, V. T. (2008). Cross-linked quaternary chitosan as an adsorbent for the removal of the reactive dye from aqueous solutions. *Journal of Hazardous Materials*, *155*, 253–260.

Singh, V., Sharma, A. K., Tripathi, D. N., & Sangh, R. (2009). Poly(methylmethacrylate) grafted chitosan: An efficient adsorbent for anionic azo dyes. *Journal of Hazardous Materials*, *161*, 955–966.

Tien, C. (1994). *Adsorption calculations and modelling. Butterworth–Heinemann Series in Chemical Engineering* Boston: Butterworth–Heinemann.

Trotmann, E. R. (1984). *Dyeing and chemical technology of textile fibres* (6th ed.). London: Charles Griffin and Company Ltd.

Weber, W. J., & Morris, J. (1963). Kinetics of adsorption on carbon from solution. *Journal of the Sanitary Engineering Division: American Society of Civil Engineers*, *89*(SA2), 31–59.

Webi, T. W., & Chakravort, R. K. (1974). Pore and solid diffusion models for fixed bed adsorbers. *AIChE Journal*, *20*, 228–238.

Wong, Y. C., Szeto, Y. S., Cheung, W. H., & McKay, G. (2003). Equilibrium studies for acid dye adsorption onto chitosan. *Langmuir*, *19*, 7888–7894.

Wu, F. C., Tseng, R. L., Huang, S. C., & Juang, R. S. (2009). Characteristics of pseudo-second order kinetic model for liquid-phase adsorption: A mini-review. *Chemical Engineering Journal*, *151*, 1–9.

Xi, K., Tabata, Y., Uno, K., Yoshimoto, M., Kishida, T., Sokawa, Y., et al. (1996). Liver targeting of interferon through pullulan conjugation. *Pharmaceutical Research*, *13*, 1846–1850.

Xu, S., Wang, J., Wu, R., Wang, J., & Li, H. (2006). Adsorption behaviors of acid and basic dyes on crosslinked amphoteric starch. *Chemical Engineering Journal*, *117*, 161–167.